


Article

Comparative Analysis of System Performance and Thermal Comfort for an Integrated System with PVT and GSHP Considering Two Load Systems: Convective Heating and Radiant Floor Heating

Sangmu Bae ¹, Yujin Nam ^{1,*} and Joon-Ho Choi ²

¹ Department of Architectural Engineering, Pusan National University, 2 Busandaehak-ro 63, Geomjeong-gu, Busan 46241, Korea; sangmu_bae@pusan.ac.kr

² School of Architecture, University of Southern California, Los Angeles, CA 90089, USA; joonhoch@usc.edu

* Correspondence: namyujin@pusan.ac.kr; Tel.: +82-51-510-7652; Fax: +82-51-514-2230

Received: 1 September 2020; Accepted: 19 October 2020; Published: 21 October 2020



Abstract: The zero-energy building (ZEB) concept has a high potential for securing energy savings in the building sector. To achieve ZEB, various active systems, including renewable systems such as photovoltaic, solar heating, and geothermal systems, have been developed. However, the existing systems are costly or not optimized. To overcome these issues, the authors previously developed an integrated tri-generation system. In this research, the previously developed system was comprehensively analyzed considering the indoor thermal comfort and energy efficiency to develop a design and operation method for the integrated system. Two different heating systems (convective heating and radiant floor heating) were employed in the tri-generation system, and their system performance, predicted mean vote (PMV), and predicted percentage of dissatisfied (PPD) were compared using simulations. The results showed that the heating coefficient of power of the radiant floor heating system was 18.8% higher than that of the convective heating system. Moreover, the radiant floor heating system (Case 4) met the PMV and PPD standards during all the heating periods. Overall, radiant floor heating was found to be more efficient than convective heating. The results confirm that radiant floor heating is more suitable than convective heating considering the indoor thermal comfort of occupants.

Keywords: tri-generation system; photovoltaic-thermal module; ground-source heat pump; convective heating; radiant floor heating; energy efficiency; thermal comfort

1. Introduction

In recent years, issues in energy saving in the building sector have become significant from the aspects of not only global warming and energy security but also economic stability. Energy cost accounts for 50% of the total heating, ventilation, and air conditioning (HVAC) system cost of the building life cycle [1]. Therefore, energy costs must be considered during the building design stage to ensure energy saving in the building sector. The zero-energy building (ZEB) concept is one of the most suitable approaches aimed at achieving this purpose. Many leading countries have actively participated in the dissemination of ZEB through policy support or financial incentives. In the U.S., Executive Order (EO) 13,834 requires all new federal buildings entering the planning process in 2020 to be designed to achieve annual reductions in building energy use and implement energy efficiency measures that reduce costs [2]. In South Korea, ZEB became mandatory for new public buildings from 2020, and this will be mandated for new private buildings by 2025 [3]. The expected market size of ZEB in Korea will also reach up to 17 billion dollars by 2024 [4]. Under this background, various active

systems, including renewable systems such as photovoltaic (PV), solar heating, and geothermal systems, have been developed and applied to achieve ZEB.

In the pursuit of ZEB, PV systems are generally applied for energy production as an active system. However, the area available for PV installation in urban buildings is often insufficient to meet the total energy requirement of the buildings. Furthermore, solar heating systems are fundamentally limited by the time gap between heat collection and heat use. A potential solution is to use a ground-source heat pump (GSHP) systems for space heating, cooling, and hot water. However, the initial cost for GSHP installation is quite high, and it requires electricity for independent operation. In an attempt to overcome the weaknesses of individual renewable systems, the authors previously developed an integrated system using multiple renewable energies and applied it in buildings [5–7]. The feasibility of the system was analyzed, and a tri-generation system integrating PV thermal collector (PVT) and GSHP was found to be acceptable with a payback period of 8 years in the market of HVAC systems if a subsidy for installation is provided [7]. Nevertheless, it is necessary to find a solution for achieving affordability and feasibility without an additional subsidy, because government policy support, such as incentives and subsidies, cannot be depended upon forever.

System feasibility depends on the building and climate conditions, because the system capacity and energy consumption of HVAC systems could also change according to the weather or building load conditions [8,9]. Papadopoulos et al. [10] suggested the optimum heating and cooling setpoint temperatures of HVAC systems for large office buildings, considering energy savings and occupant thermal comfort. For this purpose, they analyzed the potential of energy savings and thermal comfort in seven climate zones across the U.S. Kim et al. [11] investigated the indoor thermal environment induced by four HVAC systems—namely, constant air volume (CAV), variable air volume (VAV), underfloor air distribution (UFAD), and dedicated outdoor air system (DOAS). In addition, they analyzed the cooling energy consumptions and CO₂ emissions using a dynamic analysis program. As a result, the cooling energy was increased by about 23.3% when they applied CAV compared to VAV. Moreover, the CO₂ emissions were 34,679 kg of CO₂ in the VAV system and 42,400 kg of CO₂ in the CAV system. Robledo-Fava et al. [12] analyzed the influence of design value for clothing factor and human metabolic index for calculating the energy demand of buildings based on ISO 7730. Kim et al. [13] analyzed the influence of the control methods of a variable refrigerant flow (VRF) system on energy consumption and indoor thermal comfort using a simulation tool. The energy consumption of VRF using the PMV control showed a reduction of about 24% compared with the 26 °C indoor set point control. In addition, the results of thermal comfort indicated that approximately 86.8% of occupants were satisfied with acceptable thermal comfort levels. Mohelníková et al. [14] evaluated the energy consumption, indoor thermal comfort, and daylight in school buildings and found that windows are key elements influencing indoor climate and visual comfort. However, it was not of significant importance for heating energy reduction. Elhadad et al. [15] assessed the building energy and PMV for common residential houses in Egypt using simulation simplification methods considering four scenarios. All the simplification scenarios exhibited a marginal average deviation in the total energy demand and indoor thermal comfort by 20%. Park et al. [16] investigated the thermal comfort of a combined radiation-convection floor heating system through an experimental test and found that the convection heating type is inappropriate for occupants who sleep on the floor because the floor temperature is too low. In contrast, the combined radiation-convection heating type provided a thermally comfortable environment for the occupants. Fan et al. [17] evaluated the indoor thermal comfort and performance characteristics of an under-floor-air-distribution (UFAD) system under heating mode. They recommended an optimal return vent height of 1.05–1.25 m to maximize the level of indoor thermal comfort and indoor air quality with minimum energy input over a whole year.

Many studies have reported that the use of a tri-generation system for achieving occupant thermal comfort according to setpoint temperature and indoor air temperature control can be a reasonable solution to the realization of ZEB [18–21]. In this research, a tri-generation system was comprehensively analyzed to develop a method for its design and operation, considering human thermal comfort

and energy efficiency. To this end, an integrated simulation was performed with building, individual equipment, and weather models. In the integrated renewable energy system, the PVT and GSHP systems were used as energy sources, and two different heating systems were compared in terms of the system performance and PMV based on annual dynamic energy simulation.

2. Integrated Simulation Model

2.1. Overview of the Integrated Simulation Model

Figure 1 shows a summary of the integrated simulation model used in this research. The system has PVT and GSHP as heat source systems, a fan coil unit (FCU) and floor heating as space heating systems, and an FCU as a cooling system. The integrated model has a thermal storage tank for storing solar and ground heat. The building is based on ISO 13,790 and the calculation condition presented in [18]. The energy efficiency was calculated based on the total energy production and consumption by all equipment in the system. Furthermore, the PMV was calculated by the indoor air temperature, air velocity, humidity, mean radiation temperature (MRT), metabolic rate (MET), and clothing factor (Clo.), which are based on ISO 7730 [22].

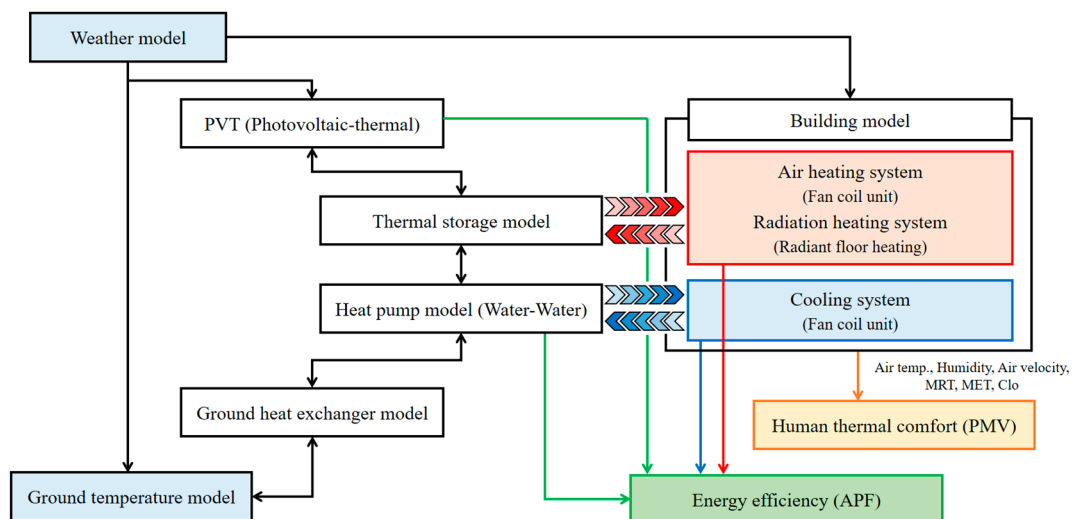


Figure 1. Summary of the integrated simulation model.

The PVT model, thermal storage model, heat pump model, and ground heat exchanger (GHX) model used in the integrated simulation are based on the tri-generation model built by the author in a previous study [7]. In this study, a convective heating system model using an FCU and a radiant floor heating system was constructed to analyze the energy efficiency and thermal comfort according to the heating type and operating conditions. Figure 2 shows a schematic of the integrated model for the convective heating system.

Figure 3 shows the control strategy of the integrated system. The integrated system is operated based on the load of the building and the indoor setpoint temperature. The operation of each unit (PVT module and heat pump) is determined by the setpoint temperature of the heat storage tank (HST) and outlet temperature of the PVT module. Figure 3 shows the control strategy of the integrated system. The control strategy includes the heating operation and heat storage operation. A heating operation is performed when the average temperature of the heat storage tank is 45 °C or higher.

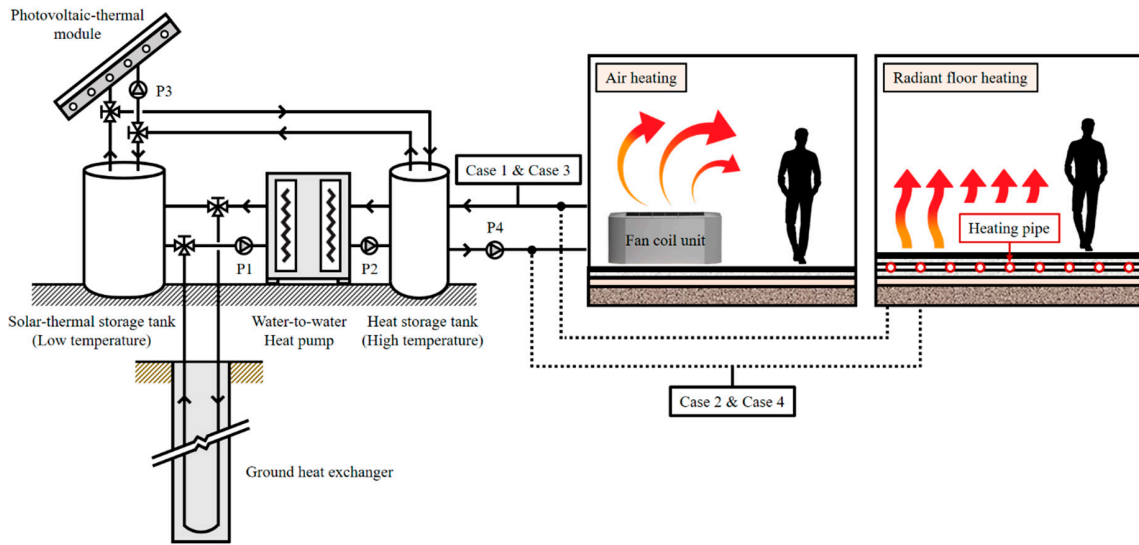


Figure 2. Schematic diagram of the integrated model for convective heating and radiant floor heating.

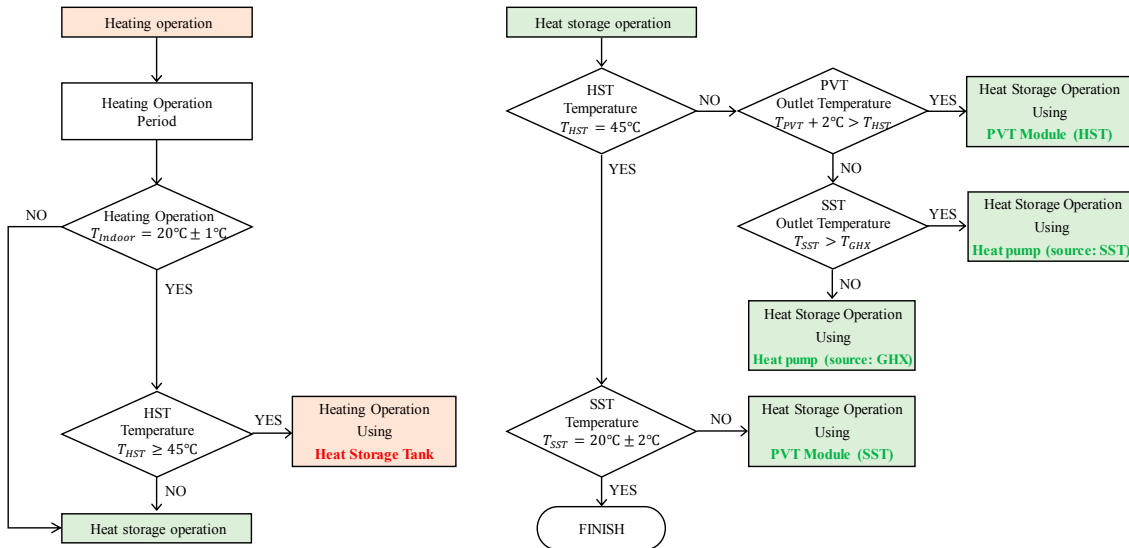


Figure 3. Control strategy of the integrated system.

The heat storage operation using the PVT module is conducted when the outlet temperature of the PVT module is 2 °C higher than the average temperature of the HST. If the heat storage operation cannot be conducted using the PVT module, the heat storage operation is performed with the heat pump. At this time, the heat pump is used the solar-thermal storage tank (SST) and GHX; the heat pump is utilized with a higher outlet temperature between SST and GHX. The PVT module stores heat to the SST when the HST average temperature is above 45 °C.

2.2. Analysis Method (Equation) of Integrated Simulation Model

Figure 4 shows the structure of the system of thermo-active construction elements. Thermo-active elements, such as the radiant floor model, are used to condition buildings by integrating a fluid system into the building.

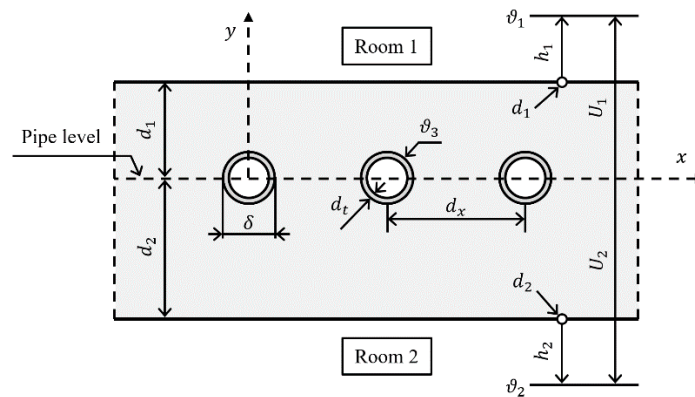


Figure 4. Schematic of the thermo-active construction element.

A two-dimensional temperature field occurs in the plane of the cross-section of the thermally active component due to the finite distance between the pipes. Thermal input or output through the pipe loop changes the water temperature in the pipe [23]. A stationary solution for the temperature distribution in the x-y plane is represented by Equation (1) for heat flow from the surface towards the indoor space:

$$q_a = \Phi \cdot U_1 \cdot (\vartheta_3 - \vartheta_1) + (1 - \Phi) \cdot \frac{U_1 \cdot U_2}{U_1 + U_2} \cdot (\vartheta_2 - \vartheta_1) \quad (1)$$

$$\Phi = \frac{2 \cdot \pi \cdot \lambda_b \cdot \Gamma}{d_x \cdot (U_1 + U_2)} \quad (2)$$

$$\Gamma = \left[\ln \left(\frac{d_x}{\pi \cdot \delta} \right) + \frac{2 \cdot \pi \cdot \lambda_b}{d_x \cdot (U_1 + U_2)} + \sum_{s=1}^{\infty} \frac{g_1(s) + g_2(s)}{s} \right]^{-1} \quad (3)$$

The calculation of MRT was defined by Fanger [24]. MRT is the uniform temperature of an imaginary enclosure in which the radiant heat transfer in the actual nonuniform enclosure. MRT varies according to the person's posture and the color of clothing for short-wave radiation, and calculates based on a person in relation to the surrounding wall and the surface temperature of the enclosure [25].

$$T_{\text{MRT}} = T_1 F_{p-1} + T_2 F_{p-2} + \dots + T_n F_{p-n}, \quad (4)$$

where T_n is the surface temperature of the area and F_p is the angular factor between a person and the area.

The calculation model of PMV is based on ASHRAE (American Society of Heating, Refrigerating and Air-Conditioning Engineers) Standard 55-2013 [26]. This PMV model can be calculated for a wide range of six parameters (air temperature, MRT, relative humidity, air velocity, Clo., and MET) based on the thermal load of a body in the environment:

$$\text{PMV} = L(0.303e^{-0.036M} + 0.028), \quad (5)$$

$$L = (M - W) - E_s - E_{re} - C_{re} - R - C, \quad (6)$$

$$M = \frac{21(0.23RQ + 0.77)Qo_2}{A_D}, \quad (7)$$

$$A_D = 0.202m^{0.425}l^{0.725}, \quad (8)$$

where PMV is the predicted mean vote, L is the thermal load, M is the metabolic rate, W is the rate of mechanical work accomplished, E_s is the total rate of evaporative heat loss from the skin, E_{re} is the rate of evaporative heat loss from respiration, C_{re} is the rate of convective heat loss from respiration, R and C

are the heat losses, RQ is the respiratory quotient, Q_{O_2} is the volumetric rate of oxygen consumption at 0°C , A_D is the DuBois surface area, m is the person's weight, and l is the person's height.

After calculating PMV, the predicted percentage dissatisfied (PPD) can also be estimated as:

$$\text{PPD} = 100 - 95e^{-0.03353\text{PMV}^4 + 0.2179\text{PMV}^2}. \quad (9)$$

In ASHRAE Standard 55-2013, the satisfaction range of PMV is ± 0.5 ($-0.5 < \text{PMV} < +0.5$), and the range of PPD is below 10% ($\text{PPD} < 10\%$) [26].

The heat pump model is based on a user-supplied file [27]. This file contains catalog data for the source-side and load-side flow rate, entering load temperature, entering source temperature, capacity, and power. The heating and cooling coefficient of performance (COP) of the heat pump can be calculated by Equations (11) and (12) [27].

$$\text{COP}_{\text{HP,heating}} = \frac{Q_{\text{absorbed}} + P_{\text{heating}}}{P_{\text{heating}}}, \quad (10)$$

$$\text{COP}_{\text{HP,cooling}} = \frac{Q_{\text{rejected}} - P_{\text{cooling}}}{P_{\text{cooling}}}, \quad (11)$$

where $\text{COP}_{\text{HP,heating}}$ is the heat pump COP in heating mode, Q_{absorbed} is the energy absorbed by the heat pump in heating mode, P_{heating} is the power drawn by the heat pump in heating mode, $\text{COP}_{\text{HP,cooling}}$ is the heat pump COP in cooling mode, Q_{rejected} is the energy rejected by the heat pump in cooling mode, and P_{cooling} is the power drawn by the heat pump in cooling mode. The heat pump is controlled by fluid flow through absorbing energy in the heating mode or rejecting energy in the cooling mode.

COP was calculated considering the total heat production and total energy consumption. The total heat production is the sum of the heat production of the photovoltaic-thermal module and the heat pump. The total energy consumption is the sum of the power consumption of the FCU, the circulating pumps, and the heat pump.

$$\text{COP}_{\text{SYS}} = \frac{Q_{\text{PVT}} + Q_{\text{HP}}}{P_{\text{FCU}} + \sum P_{\text{pump}} + P_{\text{HP}}}. \quad (12)$$

where COP_{SYS} is the coefficient of the performance of the system, Q_{PVT} is the heat production by the photovoltaic-thermal module, Q_{HP} is the heat production by the heat pump, P_{FCU} is the power consumption of the fan coil unit, $\sum P_{\text{pump}}$ is the sum of the power consumption of all circulating pumps, and P_{HP} is the power consumption of the heat pump.

The thermal and electrical performance of the PVT module model was calculated based on the solar radiation, module area, electrical efficiency, and slope. The calculation method of the PVT module model is based on the book "Solar Engineering of Thermal Process," described by Duffie and Beckman [28]. The GHX model is based on the duct ground heat storage (DST) developed by Hellstrom [29]. In addition, the heat storage tank can be modeled assuming that the tanks are made up of equal volume segments [30]. The degree of stratification and tank volume are determined by the user. More details of the system unit (PVT module, heat pump, GHX, and HST) can be found in the author's previous study [7].

3. Simulation Condition and Cases

3.1. Building Model Conditions

Figure 5 shows the floor plan of the building model. The building model was implemented utilizing the TRNSYS simulation program. The building model was based on the standard design of the low-energy residential houses proposed by the Korean Ministry of Agriculture, Food and Rural Affairs [31]. The floor area of the building model was 139.75 m^2 and the height from the floor to

the ceiling was 2.4 m. The window to wall ratio (WWR) according to the cardinal direction was 1.2% in the east, 9.9% in the north, and 14.1% in the south.

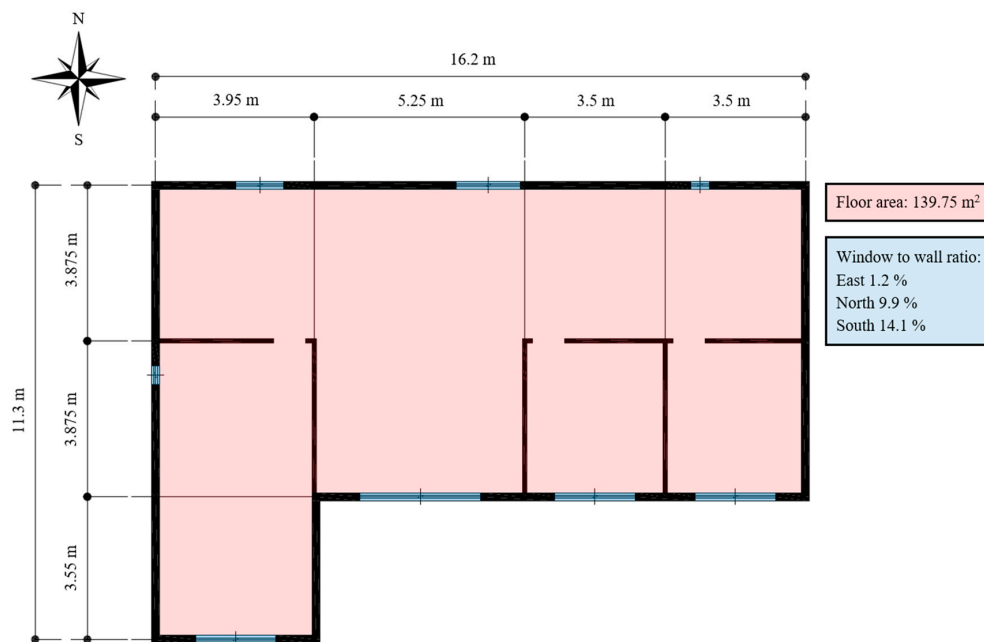


Figure 5. Floor plan of the building model.

Table 1 shows the U-values of the building model, which are based on the “Green Buildings Construction Support Act” proposed by the Korean Ministry of Land, Infrastructure, and Transport [3]. The U-values were input assuming the building model to be located in Seoul.

Table 1. U-value of the building model.

Construction Type	U-Value (W/m ² ·K)	Reference
External wall	0.242	Green Buildings Construction Support Act–2018 (Korean Ministry of Land, Infrastructure, and Transport)
Ground Floor	0.240	
Roof	0.151	
Exterior window	1.49	

Figure 6 shows the schematic diagram of the floor structure. The floor structure is composed of a finishing material, mortar, a pipe, insulation, and a concrete slab. Table 2 shows the thermal properties of the construction material.

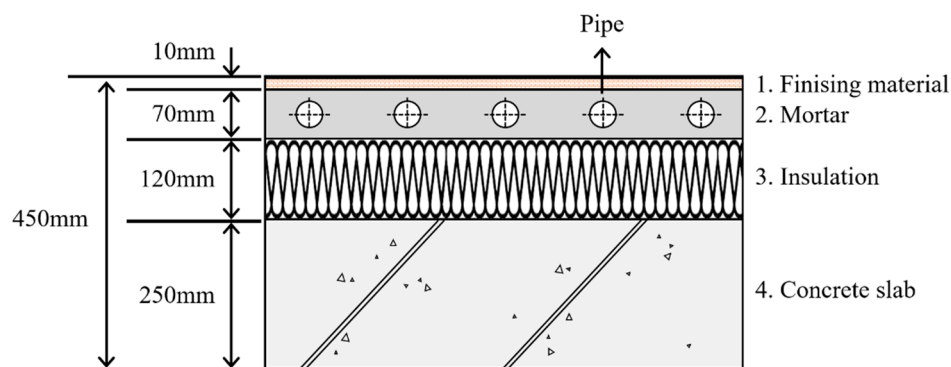


Figure 6. Schematic diagram of the floor structure.

Table 2. Thermal properties of the construction material.

Properties	Finishing	Mortar	Insulation	Concrete
Thermal conductivity (W/m·K)	0.166	1.51	0.032	1.52
Thermal capacity (kJ/kg·K)	1	0.8	1.47	0.9
Density (kg/m ³)	800	2000	30	2300

Figure 7 shows the schedules of occupants, lights, equipment, and system for a day. The schedule values of internal heat gain were based on ASHRAE 90.1-2004 [32]. The system operated for 24 h.

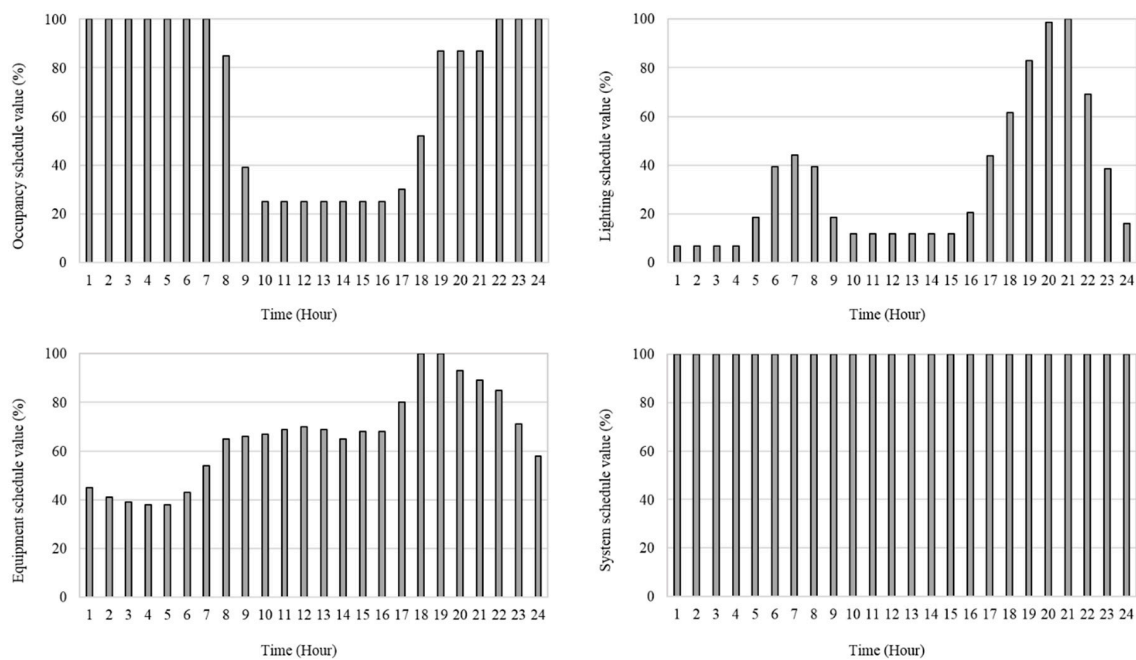
**Figure 7.** Schedule values of the internal heat gain and system.

Table 3 shows the indoor conditions of the building model. The occupants were assumed to be seated and relaxed. The number of occupants was set to four, considering the floor area. In addition, the lighting power density (LPD), equipment power density (EPD), and infiltration were set based on ASHRAE 90.1-2004 and ASHRAE 90.2-2004 [33].

Table 3. Indoor conditions of the building model.

Parameter	Value	Reference
People	Sensible heat 75 W Latent heat 45 W	ASHRAE Standard 55-2013
Light	10.76 W/m ²	ASHRAE Standard 90.1-2004
Equipment	9.68 W/m ²	ASHRAE Standard 90.1-2004
Infiltration	0.5 ACH	ASHRAE Standard 90.2-2004

Table 4 shows the thermal comfort conditions. The occupants, who were wearing simple clothes, were assumed to be seated and relaxed.

Table 4. Thermal comfort conditions.

Parameter	Value	Reference
Clothing factor	Winter 1.0 Clo., Summer 0.5 Clo.	ASHRAE Standard 55-2013
Metabolic rate	1 MET	
Air velocity	0.1 m/s	

3.2. Simulation Cases

In this study, a case study was conducted on the heating type and operating conditions. Table 5 shows the case study conditions. The heating type was classified as (1) the convective heating system using FCU and (2) the radiant floor heating system. Thermal comfort, according to the heating type, was analyzed through Case 1 and Case 2. The indoor setpoint temperatures for Case 1 and Case 2 were based on the ASHRAE 90.2-2004 single zone [33]. Case 3 and Case 4 focused on the thermal comfort of the occupant rather than the energy efficiency of the system. For the indoor setpoint temperatures for Case 3 and Case 4, the range of comfortable heating and cooling temperatures suggested by ASHRAE standard 55-2013 was considered [26].

Table 5. Case study conditions.

	Heating Type	Indoor Setpoint Temperature	Reference
Case 1	Convective heating	Heating 20 °C	ASHRAE 90.2-2004
Case 2	Radiant floor heating		
Case 3	Convective heating	Heating 22 °C	ASHRAE standard 55-2013
Case 4	Radiant floor heating		

4. Simulation Result

4.1. Building Load

Figure 8 shows the ambient temperature of Seoul and the monthly energy demand of the building model. The annual average temperature in Seoul is 11.8 °C; the minimum is −14.5 °C and the maximum is 33.8 °C. The annual heating and cooling loads were calculated to be 11,039 kWh and 1335 kWh, respectively. Furthermore, the heating and cooling peaks were 9.35 and 2.72 kW, respectively. Therefore, the building model of the case study was assumed to be a heating-dominant building. The system capacity of each component was set according to the results of load calculation, and Table 6 presents the specific information of the system.

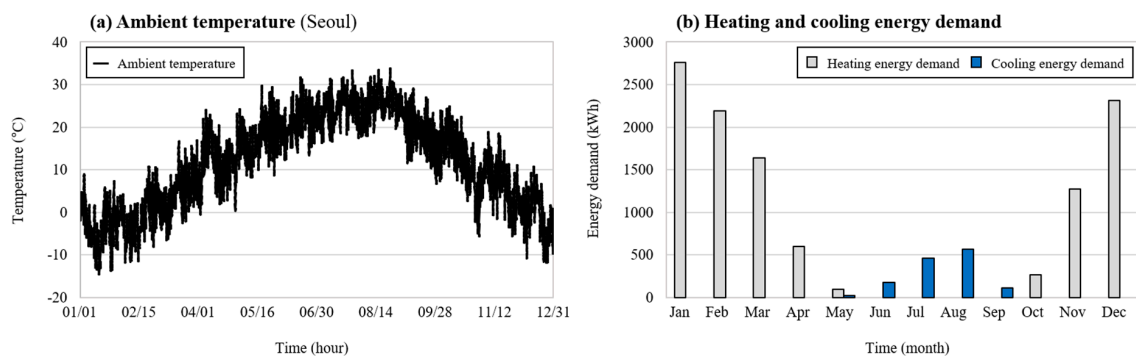
**Figure 8.** Ambient temperature and energy demand of the building model.

Table 6. Component conditions of the integrated simulation model.

Component	Name	Value
PVT collector	Type	Unglazed water
	Length and width	1.01 m × 19.72 m (19.95 m ²)
	Number of tubes	210
	PV efficiency	20%
	Slope	35°
Heat pump	Type	Water-to-water
	Heating capacity	10.5 kW
	Cooling capacity	11.3 kW
Ground heat exchanger	Number of boreholes	1
	Borehole radius	0.15 m
	Borehole depth	200 m
Circulating pump	Number of pumps	5
	Power consumption	2 kW
Fan coil unit (Convective heating)	Heating capacity	15 kW
	Cooling capacity	12 kW
	Fan power	0.09 kW
Floor heating pipes (Radiant floor heating)	Pipe spacing	0.2 m
	Pipe outside diameter	0.02 m
	Pipe wall thickness	0.001 m
	Pipe wall conductivity	1.36 kJ/h·m·K

4.2. Energy Efficiency

4.2.1. Thermal and Electric Performance on a Representative Day

Figure 9 shows the thermal and electrical performance of the system on a representative day (January 28) in winter. The heat exchange rate (HER) of the heat pump was calculated as 105 and 110 kW for convective heating (Case 1) and radiant floor heating (Case 2), respectively. There was no significant difference in the amount of heat and electricity produced by the PVT collector according to the heating type.

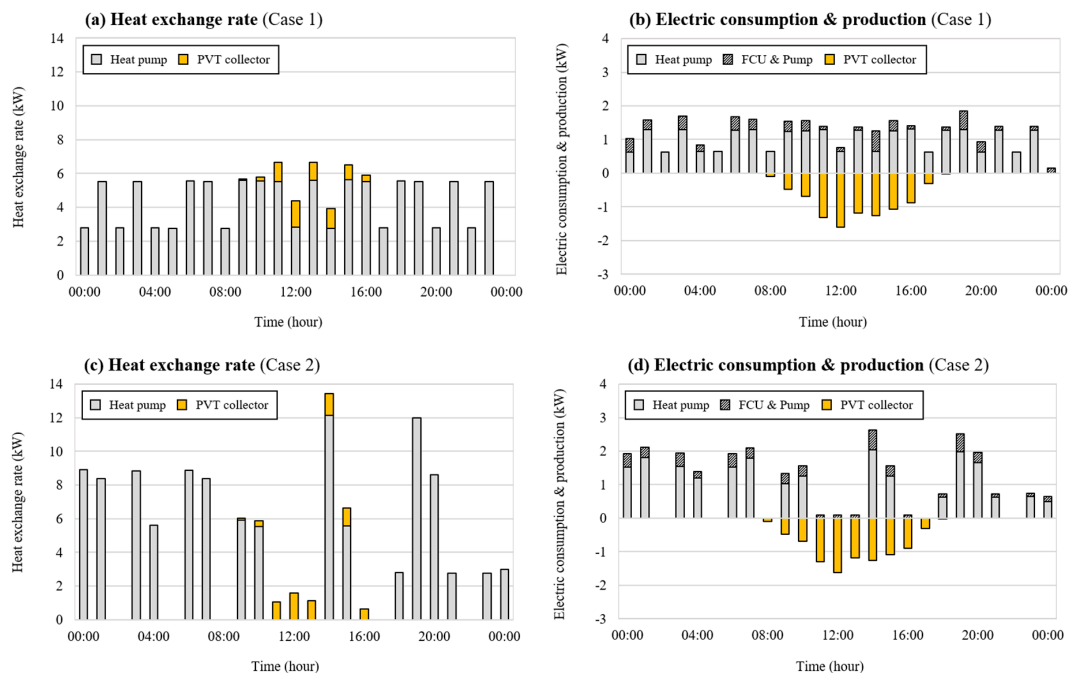


Figure 9. Thermal and electric performance on a representative day in winter (Case 1 and Case 2).

Under the same heating load condition, the convective heating (Case 1) system operated continuously, and the radiant floor heating (Case 2) system operated intermittently. The electricity consumption of the heat pump was calculated as 24.3 kW for convective heating (Case 1) and 20.9 kW for radiant floor heating (Case 2). The operation time of the heat pump was 50% longer for convective heating than for radiant floor heating. More heat was produced via radiant floor heating than via convective heating, although the operating time of the heat pump was shorter.

Figure 10 shows the COP of the heat pump on a representative day for heating. The average COP of the heat pump on the representative day of heating was calculated as 4.3 and 5.2 for convective heating (Case 1) and radiant floor heating (Case 2), respectively. The heating COP of radiant floor heating was 18.8% higher than that of convective heating, indicating that the heating performance of the heat pump of the radiant floor heating was more efficient. For the cooling COP, there was no difference between the two systems.

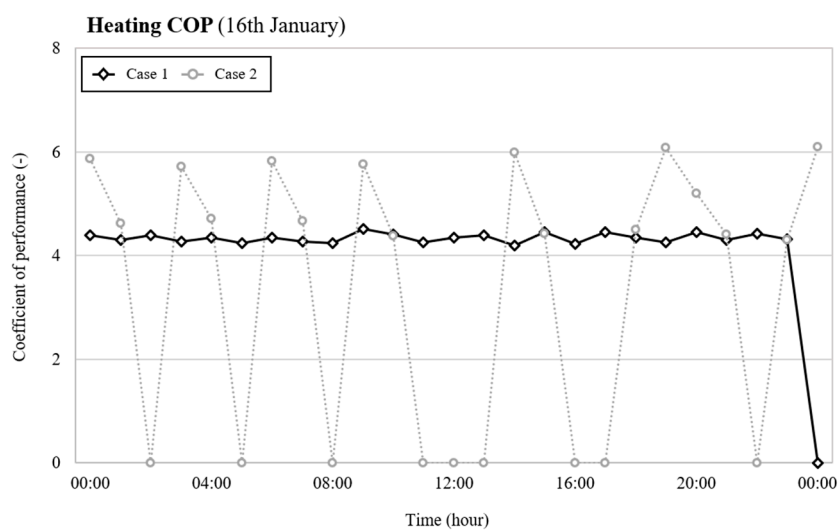


Figure 10. Heating COP of the heat pump on a representative day (Case 1 and Case 2).

4.2.2. Weekly Performance of Heat Pump and System

Figure 11 shows the HER, electric consumption, heat pump COP, and system COP from January 12 to January 18. The average COP of the heat pumps for convective heating (Case 1 and Case 3) and radiant floor heating (Case 2 and Case 4) was calculated as 4.3, 5.3, 4.3, and 5.3, respectively. The average COP of the system for convective heating (Case 1 and Case 3) and radiant floor heating (Case 2 and Case 4) was calculated as 3.5, 4.5, 3.5, and 4.5, respectively. The heating type had a more substantial influence on the COP of the heat pump and the system than the indoor set temperature. Table 7 shows a summary of the average COP in Figure 11c,d.

4.2.3. Monthly Performance of Heat Pump and System

Figure 12 shows the monthly performance of the heat pump and the system. The average COP of the heat pump in the winter season was calculated as 4.6, 5.4, 4.6, and 5.4 from Case 1 to Case 4, respectively. In addition, the average system COP was calculated as 4.5, 5.3, 4.3, and 5.2. The heating performance varied with the heating type. The heat pump COP and system COP for radiant floor heating were 18.7% and 21.8% higher than those for convective heating. These results clearly show the advantage of radiant floor heating over convective heating in terms of the HER and electricity consumption (operation time), as shown in Figure 9.

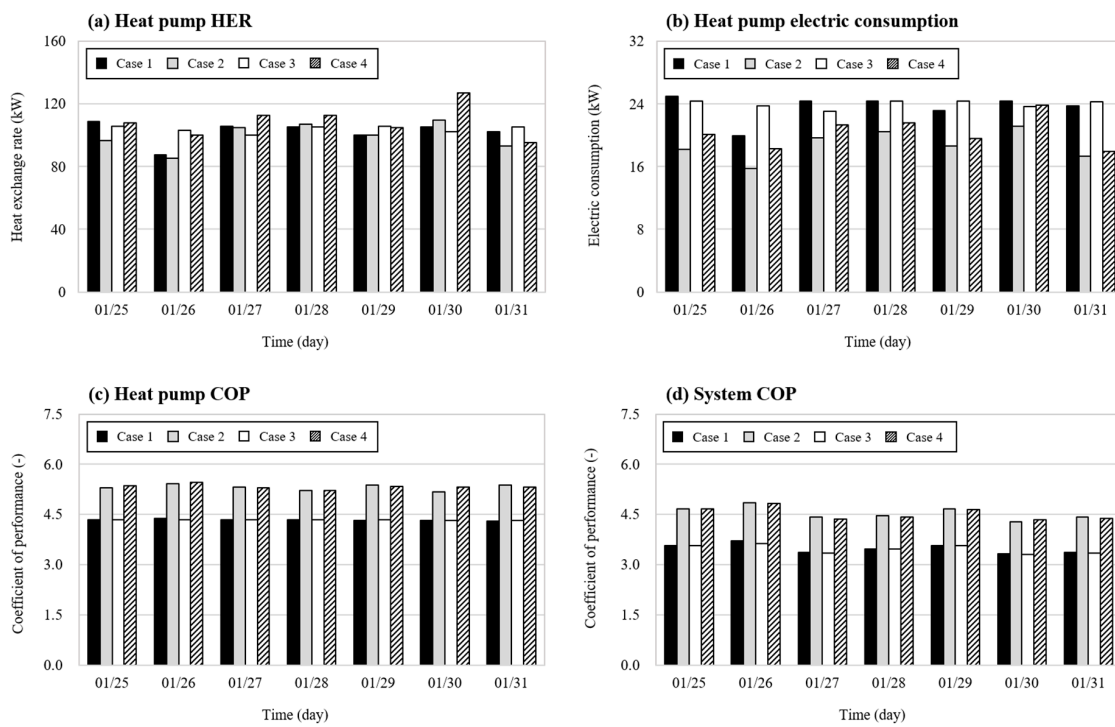


Figure 11. Weekly performance of the heat pump and system.

Table 7. Average COP of the heat pump and system on a week.

	Heat Pump COP	System COP
Case 1	4.3	3.5
Case 2	5.3	4.5
Case 3	4.3	3.5
Case 4	5.3	4.5

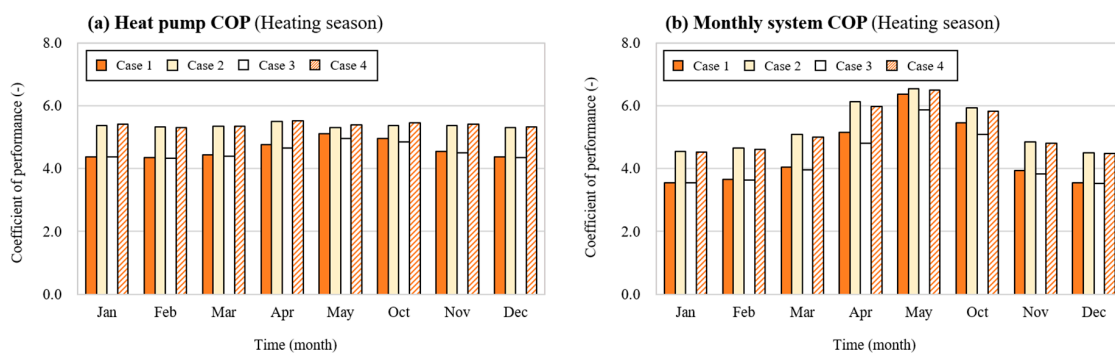


Figure 12. Monthly performance of the heat pump and system.

4.3. Indoor Thermal Comfort

4.3.1. Thermal Environmental Parameters

Figure 13a shows the indoor air temperatures (T_a) of convective heating and radiant floor heating on a representative day in winter (28 January). The indoor air temperature of convective heating was calculated as 21.9 °C and 22.2 °C for Case 1 and Case 3, respectively. In addition, the indoor air temperature of radiant floor heating was calculated as 19.9 °C and 21.9 °C for Case 2 and Case 4, respectively. For radiant floor heating, the indoor air temperature was confirmed to be similar to

the indoor setpoint temperature. For convective heating, the indoor air temperature was similar to or higher than the indoor setpoint temperature.

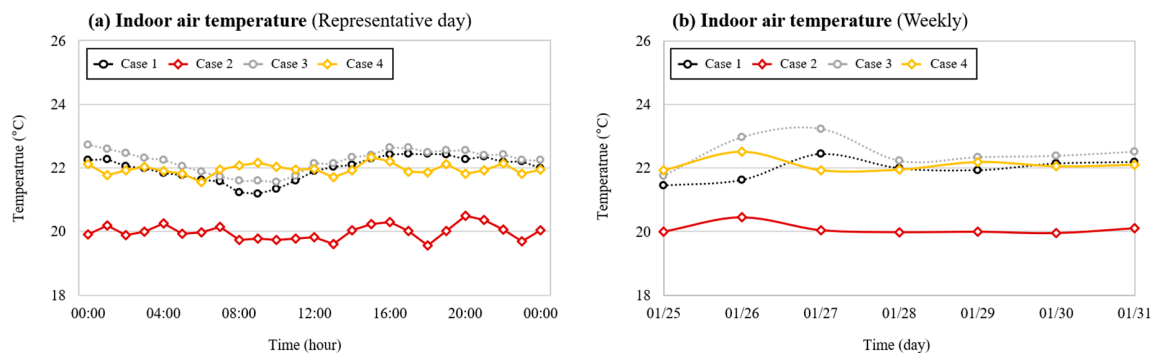


Figure 13. Indoor air temperature on a representative day and week.

Figure 13b shows the indoor air temperatures (T_a) of the convective heating and radiant floor heating for a week period (January 25–31). Convective heating exhibited a larger variation in indoor air temperature than radiant floor heating. On the other hand, the indoor air temperature of the radiant floor heating is almost constant. This is because the heat output from the heated floor is controlled according to the indoor air temperature due to the self-control effect of radiant floor heating [34].

Figure 14a shows the MRT on a representative day. Changes in the MRT of convective heating and radiant floor heating were similar to those of indoor air temperature (Figure 12). For radiant floor heating, MRT was higher than the indoor air temperature by approximately 1.3 °C. In contrast, for convective heating MRT was lower than the indoor air temperature by approximately 1.4 °C.

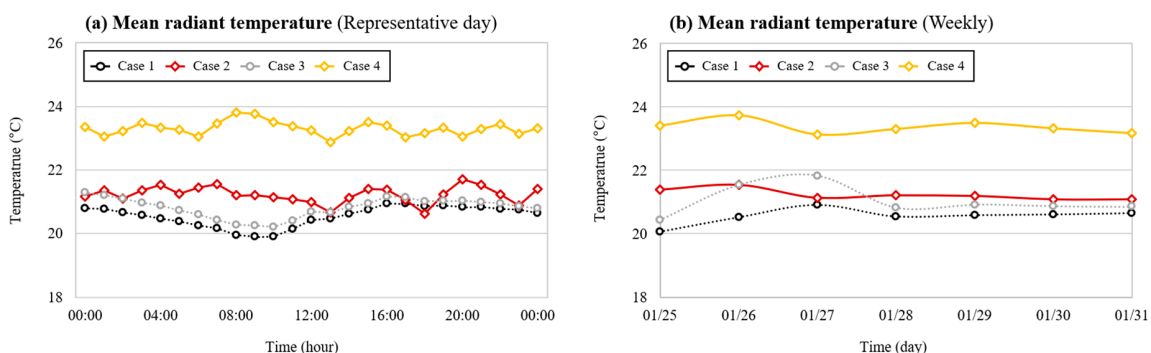


Figure 14. Mean radiant temperature (MRT) on a representative day and week.

Figure 14b shows the MRT for a week. For convective heating, the average MRT during the week was calculated as 20.6 and 21.0 °C in Case 1 and Case 3, respectively. For radiant floor heating, the corresponding values were 21.2 and 23.4 °C. The MRT exhibited a variation according to the heating type. The MRT of Case 4 increased by 2.3 °C compared to Case 3. The radiant floor heating system is a higher MRT than the convective heating system because of the increased radiant heat exchange.

Figure 15a shows the monthly average indoor air temperature (T_a) for one year. For convective heating, the indoor air temperature was higher than the indoor set-point temperature by approximately 1 °C. This is because the convective heating system can supply high-temperature heat to the zone in a short time compared to the radiant floor heating system. In contrast, for radiant floor heating, the indoor air temperatures were 20.6 and 22.3 °C in Case 2 and Case 4, respectively.

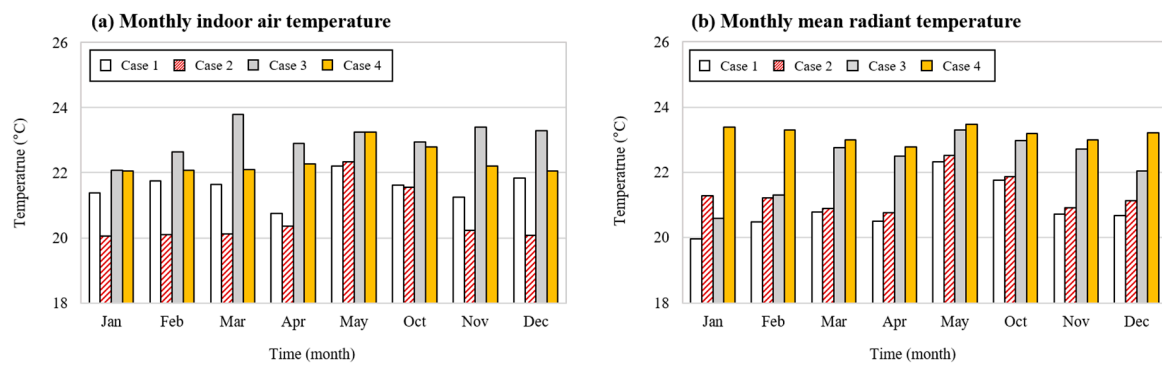


Figure 15. Monthly indoor air temperature and mean radiant temperature (MRT).

Figure 15b shows the monthly average MRT for one year. The changes in MRT, according to the heating type, were more pronounced at higher heating loads (January, February, and December). This is because the radiant floor heating system takes more time to heat the floor structure and supply radiant heat to the space at a higher heating load. On the other hand, the MRT was similar for radiant floor heating and convective heating at low heating loads (April, May, and September).

4.3.2. Indoor Thermal Comfort

Figure 16a shows the PMV on a representative day. The red line represents the one of the ranges of the PMV standard ($-0.5 < PMV < 0.5$) proposed by ASHRAE Standard 55-2013 [22]. The cases of convective heating show that the PMV was below -0.5 throughout the day and did not reach the thermal comfort zone. PMV was higher with radiant floor heating than with convective heating. In particular, the average PMV of Case 4 for radiant floor heating met the thermal comfort zone.

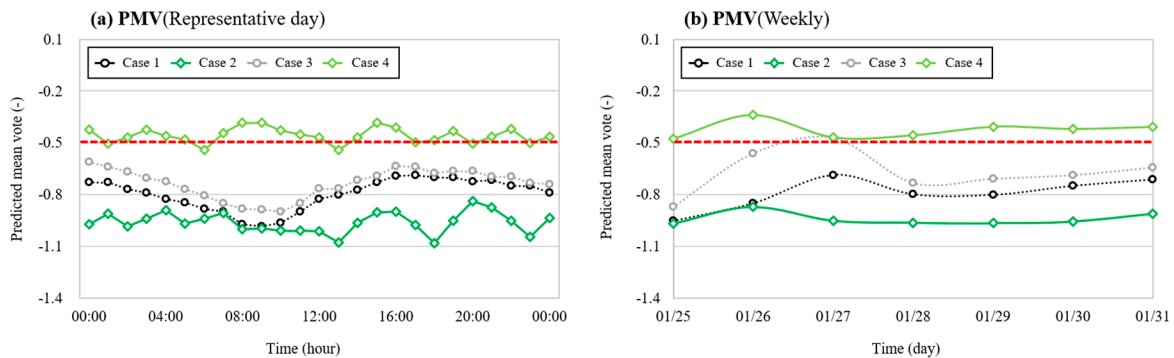


Figure 16. Predicted mean vote (PMV) on a representative day and week.

Figure 16b shows PMV for a week. The average PMVs in Case 1 to Case 4 were estimated at -0.8 , -0.9 , -0.7 , and -0.4 , respectively. The MRT levels for radiant floor heating (Case 2) and convective heating (Case 3) were similar; however, the PMV was higher for convective heating (Case 3) than for radiant floor heating (Case 2). Despite the higher MRT, the PMV decreased with a decreasing indoor air temperature. On the other hand, convective heating (Case 3) reached a period of satisfying PMV on January 27. However, most other periods did not meet the PMV standard. Radiant floor heating (Case 4) satisfied the PMV for a week. These results confirm that the radiant floor heating system is superior to the convective heating system in terms of indoor thermal comfort.

Figure 17a shows the predicted percentage of dissatisfied (PPD) on a representative day. The red line represents the PPD standard ($PPD < 10\%$) suggested by ASHRAE Standard 55-2013 [22]. From Case 1 to Case 4, the PPDs were 18.6%, 24.6%, 16.5%, and 9.5%, respectively. With radiant floor heating

(Case 4), though the PPD standard (PPD < 10%) was exceeded once, the standard was sustained throughout the most of the time.

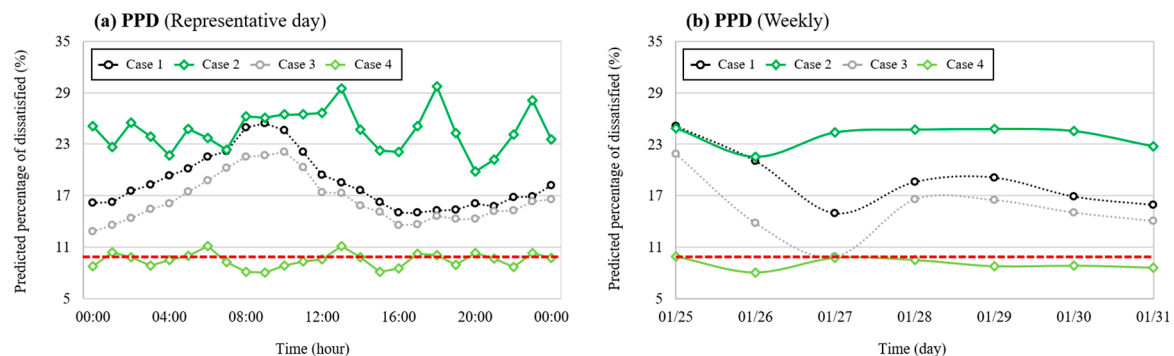


Figure 17. Predicted percentage of dissatisfied (PPD) on a representative day and week.

Figure 17 shows the PPD for a week. For convective heating (Case 3), the standard was met once but was not satisfied during the remaining period. The radiant floor heating system satisfied the PPD standard only when the indoor set-point temperature was 22 °C. Even when the indoor air temperature reached a generally acceptable level, it hardly met the PPD standard at a low MRT.

Figure 18a illustrates the monthly average PMV. Neither convective heating (Case 1) nor radiant floor heating (Case 2) met the PMV standard during the heating periods, except in May and October, when the heating load was low. Meanwhile, convective heating (Case 3) did not meet the PMV standard, even though the average indoor air temperature exceeded 22 °C in January and February. In contrast, radiant floor heating (Case 4) met the PMV standard during all the heating periods. The convective heating system did not meet the PMV standard due to the low MRT.

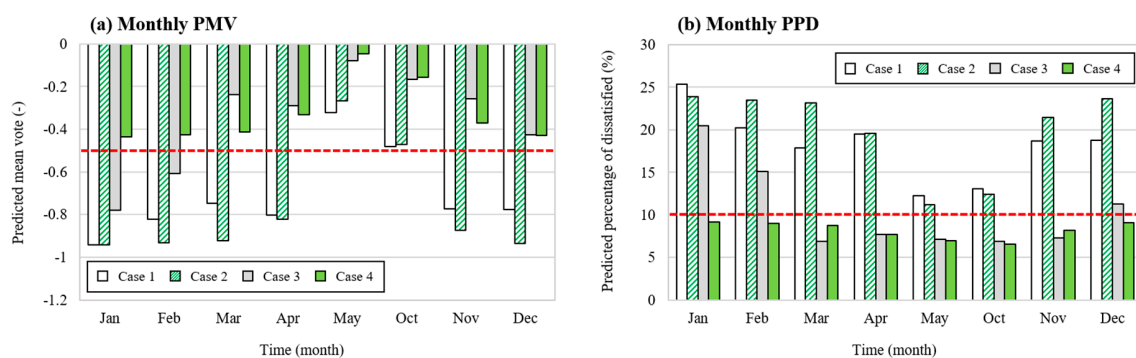


Figure 18. Monthly predicted mean vote (PMV) and predicted percentage of dissatisfied (PPD).

Figure 18b summarizes the monthly average PPD. Both convective heating (Case 1) and radiant floor heating (Case 2) failed to meet the required PPD standard during all the heating periods. Convective heating (Case 3) did not meet the required PPD either in January, February, or December, whereas radiant floor heating (Case 4) met the PPD criteria in all the heating periods. This result confirms that radiant floor heating is more suitable for the indoor thermal comfort of occupants than convective heating.

5. Conclusions

An integrated simulation was performed to develop the design and operation method for a renewable energy system considering the indoor thermal comfort and energy efficiency. The energy efficiency and indoor thermal comfort of two different heating systems were compared based on dynamic energy simulations. The conclusions of this study can be summarized as follows.

- (1) The average COPs of the heat pump on a representative day in the winter season were 4.3 and 5.2 for convective heating (Case 1) and radiant floor heating (Case 2), respectively. The heating COP for radiant floor heating was 18.8% higher than that for convective heating. Overall, the radiant floor heating system was more efficient than the convective heating system.
- (2) The radiant floor heating system was more effective for MRT than the convective heating system. The MRT showed a difference of 2.3 °C according to the heating type. The MRT difference was larger in January, February, and December, when the heating load was high. This is because the available time for radiant floor heating to heat the floor structure increased with the increasing heating load. However, the MRT was similar for both radiant floor heating and convective heating at low heating loads.
- (3) Although the MRT was higher for radiant floor heating (Case 1) than for convective heating (Case 3), the PMV standard ($-0.5 < PMV < 0.5$) was not met when the indoor air temperature was low. This result confirms that MRT has a strong influence on PMV only if an appropriate level of indoor air temperature (22 °C) is secured. For convective heating (Case 3), the standards of PMV and PPD were not met in January and February when the heating load was high. For radiant floor heating (Case 4), the PMV and PPD standards were met in all heating periods. This result confirms that the radiant floor heating system is more suitable than the convective heating system for the indoor thermal comfort of occupants.

Author Contributions: The authors S.B. and Y.N. wrote the full manuscript and comparatively analyzed the energy efficiency between convective heating and radiant floor heating. The author J.-H.C. analyzed the thermal comfort according to the heating type of the tri-generation system and reviewed this manuscript. All authors have read and agreed to the published version of the manuscript.

Funding: This work was supported by the Financial Supporting Project of Long-term Overseas Dispatch of PNU's Tenure-track Faculty, 2019.

Conflicts of Interest: The authors declare no conflict of interest.

Nomenclature

Symbols

q_a	Heat flow [W]
U	Coefficient of thermal transmittance [-]
d	distance, thickness [m]
s	Time constant [-]
T_a	The air temperature [K]
T_{MRT}	The mean radiant temperature [K]
T_n	The surface temperature of the area [K]
F_p	The angular factor between a person and the area [-]
PMV	Predicted mean vote [-3 to 3]
L	Thermal load [W/m^2]
M	Metabolic rate [W/m^2]
W	Rate of mechanical work accomplished [W/m^2]
E_s	Total rate of evaporative heat loss from skin [W/m^2]
E_{re}	Rate of evaporative heat loss from respiration [W/m^2]
C_{re}	Rate of convective heat loss from respiration [W/m^2]
R	Sensible heat loss from skin [W/m^2]
C	Sensible heat loss from skin [W/m^2]
RQ	Respiratory quotient [W/m^2]
Q_{O_2}	Volumetric rate of oxygen consumption at conditions of 0 °C [W/m^2]
A_D	DuBois surface area [m^2]
m	Person's weight [kg]
l	Person's height [m]
PPD	Predicted percentage of dissatisfied [%]

$COP_{HP,heating}$	The heat pump coefficient of performance in heating mode [-]
$COP_{HP,cooling}$	The heat pump coefficient of performance in cooling mode [-]
$Q_{absorbed}$	The energy absorbed by the heat pump in heating mode [W]
$Q_{rejected}$	The energy rejected by the heat pump in cooling mode [W]
$P_{heating}$	The power drawn by the heat pump in heating mode [W]
$P_{cooling}$	The power drawn by the heat pump in cooling mode [W]
COP_{SYS}	The system coefficient of performance [-]
Q_{PVT}	The heat production by photovoltaic-thermal module [W]
Q_{HP}	The heat production by heat pump [W]
P_{FCU}	The power consumption of fan coil unit [W]
P_{pump}	The power consumption of circulating pump [W]
P_{HP}	The power consumption of heat pump [W]

Greek Symbols

Φ	Correction factor [-]
ϑ_1	Room 1 temperature [K]
ϑ_2	Room 2 temperature [K]
ϑ_3	Outside surface temperature of the pipe [K]
δ	Outside diameter of the pipe [m]
λ_b	Thermal conductivity of material [W/m·K]

Acronyms and abbreviations

ZEB	Zero-energy building
MRT	Mean radiant temperature
PMV	Predicted mean vote
PPD	Predicted percentage of dissatisfied
COP	Coefficient of performance
PVT	Photovoltaic-thermal
GHX	Ground heat exchanger
SST	Solar-thermal storage tank
HST	Heat storage tank
FCU	Fan coil unit

References

1. National Institute of Building Sciences. *Life-Cycle Cost Analysis (LCCA)*; National Institute of Building Sciences: Washington, DC, USA, 2016.
2. Executive Office of the President. *Executive Order 13834 Efficient Federal Operations*; Executive Office of the President: Washington, DC, USA, 2018.
3. Korea Land, Infrastructure and Transport. *Green Buildings Construction Support Act*; Korea Land, Infrastructure and Transport: Sejong, Korea, 2018.
4. Korea Heating Air-Conditioning Refrigeration & Renewable Energy News (Kharn). Available online: <https://www.kharn.kr/mobile/article.html?no=11399> (accessed on 18 August 2020).
5. Jeong, Y.D.; Yu, M.G.; Nam, Y. Feasibility Study of a Heating, Cooling and Domestic Hot Water System Combining a Photovoltaic-Thermal System and a Ground Source Heat Pump. *Energies* **2017**, *10*, 1243. [CrossRef]
6. Bae, S.; Jeong, Y.; Nam, Y. Performance Analysis of Hybrid System with PVT and GSHP for Zero Energy Building. *KIEAE J.* **2018**, *18*, 85–92. [CrossRef]
7. Bae, S.; Nam, Y.; Cunha, I.D. Economic Solution of the Tri-generation System Using Photovoltaic-Thermal and Ground Source Heat Pump for Zero Energy Building (ZEB) Realization. *Energies* **2019**, *12*, 3304. [CrossRef]
8. Jeong, Y.D.; Nam, Y.; Yeo, S. Dynamic Energy Simulation for Suitable Capacity Decision of GSHP-PVT Hybrid System. *J. Archit. Inst. Korea Struct. Constr.* **2017**, *33*, 53–61.
9. Bae, S.; Nam, Y. Study on the Optimal Capacity Design for Tri-generation System using PVT and GSHP. *Trans. Korea Soc. Geotherm. Energy Eng.* **2019**, *15*, 16–23.

10. Papadopoulos, S.; Kontokosta, C.E.; Vlachokostas, A.; Azar, E. Rethinking HVAC temperature setpoints in commercial buildings: The potential for zero-cost energy savings and comfort improvement in different climates. *Build. Environ.* **2019**, *155*, 350–359. [CrossRef]
11. Kim, C.H.; Lee, S.E.; Lee, K.H.; Kim, K.S. Detailed Comparison of the Operational Characteristics of Energy-Conserving HVAC Systems during the Cooling Season. *Energies* **2019**, *12*, 4160. [CrossRef]
12. Robledo-Fava, R.; Hernández-Luna, M.C.; Fernández-de-Córdoba, P.; Michinel, H.; Zaragoza, S.; Castillo-Guzman, A.; Selvas-Aguilar, R. Analysis of the Influence Subjective Human Parameters in the Calculation of Thermal Comfort and Energy Consumption of Buildings. *Energies* **2019**, *12*, 1531. [CrossRef]
13. Kim, J.; Song, D.; Kim, S.; Park, S.; Choi, Y.; Lim, H. Energy-Saving Potential of Extending Temperature Set-Points in a VRF Air-Conditioned Building. *Energies* **2020**, *13*, 2016. [CrossRef]
14. Mohelníková, J.; Novotný, M.; Mocová, P. Evaluation of School Building Energy Performance and Classroom Indoor Environment. *Energies* **2020**, *13*, 2489. [CrossRef]
15. Elhadad, S.; Radha, C.H.; Kistelegdi, I.; Baranyai, B.; Gyergyák, J. Model Simplification of Energy and Comfort Simulation Analysis for Residential Building Design in Hot and Arid Climate. *Energies* **2020**, *13*, 1876. [CrossRef]
16. Park, B.; Ryu, S.R.; Cheong, C.H. Thermal Comfort Analysis of Combined Radiation-Convection Floor Heating System. *Energies* **2020**, *13*, 1420. [CrossRef]
17. Fan, Y.; Li, X.; Zheng, M.; Weng, R.; Tu, J. Numerical Study on Effects of Air Return Height on Performance of an Underfloor Air Distribution System for Heating and Cooling. *Energies* **2020**, *13*, 1070. [CrossRef]
18. Yang, L.; Yan, H.; Lam, J.C. Thermal comfort and building energy consumption implications—A review. *Appl. Energy* **2014**, *115*, 164–173. [CrossRef]
19. Belussi, L.; Barozzi, B.; Bellazzi, A.; Danza, L.; Devitofrancesco, A.; Fanciulli, C.; Ghellere, M.; Guazzi, G.; Meroni, I.; Salamone, F.; et al. A review of performance of zero energy buildings and energy efficiency solutions. *J. Build. Eng.* **2019**, *25*, 100772. [CrossRef]
20. Ng, L.; Poppendieck, D.; Stuart Dols, W.; Dougherty, B.P. Nist net-zero energy residential test facility. *ASHRAE J.* **2018**, *60*, 12–19.
21. Lee, E.J.; Kang, E.C.; Lee, K.S.; Ghorab, M.; Yang, L.; Entchev, E. PVT-GSHP hybrid tri-generation system for zero energy buildings. In Proceedings of the ISES Solar World Congress 2017, Abu Dhabi, UAE, 29 October 2017; Available online: <http://proceedings.ises.org/paper/swc2017/swc2017-0061-Lee> (accessed on 19 September 2020).
22. International Organization for Standardization (ISO). *Ergonomics of the Thermal Environment—Analytical Determination and Interpretation of Thermal Comfort Using Calculation of the PMV and PPD Indices and Local Thermal Comfort Criteria*; ISO 7730; ISO: Geneva, Switzerland, 2005.
23. TRNSYS 18. *Multizone Building Modeling with Type 56 and TRNBuild*; TESS Libs 18: Milwaukee, WI, USA, 2017; Volume 5.
24. Fanger, P.O. *Thermal Comfort: Analysis and Application in Environment Engineering*; McGraw Hill: New York, NY, USA, 1972.
25. International Organization for Standardization. *Ergonomics of the Thermal Environment—Instruments for Measuring Physical Quantities*; ISO 7726; ISO: Geneva, Switzerland, 2001.
26. ASHRAE. *Thermal Environmental Conditions for Human Occupancy*; ASHRAE Standard 55-2013; ASHRAE: Atlanta, GA, USA, 2013.
27. TRNSYS 17. *GHP Library Mathematical Reference*; TESS Libs 17: Milwaukee, WI, USA, 2012; Volume 4.
28. Duffie, J.A.; Beckman, W.A. *Solar Engineering of Thermal Process*, 4th ed.; John Wiley & Sons, Inc.: Hoboken, NJ, USA, 2013.
29. Hellström, G. *Duct Ground Heat Storage Model Manual for Computer Code*; Department of Mathematical Physics, University of Lund: Lund, Sweden, 1989.
30. TRNSYS 17. *Mathematical Reference*; TESS Libs 17: Milwaukee, WI, USA, 2014; Volume 4.
31. Beginning Farmers Center. Available online: www.returnfarm.com (accessed on 8 August 2020).
32. ASHRAE. *Energy Standard for Buildings Except Low-Rise Residential Buildings*; ASHRAE Standard 90.1-2004; ASHRAE: Atlanta, GA, USA, 2004.

33. ASHRAE. *Energy-Efficient Design of Low-Rise Residential Buildings*; ASHRAE Standard 90.2-2004; ASHRAE: Atlanta, GA, USA, 2004.
34. Olsen, B.W. Radiant floor heating in theory and practice. *ASHRAE J.* **2002**, *44*, 19–24.

Publisher’s Note: MDPI stays neutral with regard to jurisdictional claims in published maps and institutional affiliations.



© 2020 by the authors. Licensee MDPI, Basel, Switzerland. This article is an open access article distributed under the terms and conditions of the Creative Commons Attribution (CC BY) license (<http://creativecommons.org/licenses/by/4.0/>).